Available online at www.sciencedirect.com
ScienceDirect
International Journal of Pharmaceutics 353 (2008) 223–232
INTERNATIONAL JOURNAL OF PHARMACEUTICS
www.elsevier.com/locate/ijpharm

Pharmaceutical Nanotechnology

Study on the hydatid cyst membrane: Permeation of model molecules and interactions with drug-loaded nanoparticles

Tri Truong Cong [a], Vincent Faivre [a,*], Tien Thanh Nguyen [a], Hernan Heras [a], Fabrice Pirot [a], Nadia Walchshofer [b], Marie-Elisabeth Sarciron [c], Françoise Falson [a]

[a] *Laboratoire de Pharmacie Galénique Industrielle, ISPB – Université Lyon I, 8 avenue Rockefeller, 69373 Lyon cedex 08, France*
[b] *ISPB, Université de Lyon, Université Lyon I, 8 avenue Rockefeller, 69373 Lyon cedex 08, France*
[c] *Laboratoire de Parasitologie-Mycologie Médicale, Université Claude Bernard, Lyon I, 8 avenue Rockefeller, 69373 Lyon cedex 08, France*

Received 25 July 2007; received in revised form 5 November 2007; accepted 8 November 2007
Available online 16 January 2008

Abstract

The success of the chemotherapeutic treatment of hydatid disease is based upon the drug ability to operate on the germinal layer and on the protoscolices of the hydatid cyst interior at adequate concentrations for sufficient periods. The goal of this study was to evaluate the ability of the drug diffusion through the cyst membrane from sheep hydatid cysts and the increase of drug concentration in the cyst environment. In the first part of this work, the permeation behaviour through the hydatid cyst membrane was studied with five model molecules, having different molecular descriptors (log *P*, molecular weight, polar surface area . . .) onto static Franz glass diffusion cells. A good correlation has been observed between the permeation coefficient and the partition coefficient, log *P* ($r = 0.951$). In the second part, albendazole-loaded nanoparticles (about 300 nm) prepared by the emulsion solvent evaporation method have shown a sufficient entrapment efficiency ($36.4 \pm 6.4\%$) to raise the apparent solubility of albendazole. The diffusion of drug from the nanoparticles across the hydatid cyst membrane was also improved compare to albendazole suspension. These results have shown the interest of the albendazole-loaded nanoparticles for the treatment of hydatid cysts in the future.
© 2007 Elsevier B.V. All rights reserved.

Keywords: *Echinococcus granulosus*; Hydatid cyst; Diffusion; Nanoparticles; Albendazole

1. Introduction

Hydatid disease caused by *Echinococcus granulosus* is a major zoonotic infection that is detrimental to both human health and animal husbandry in many endemic areas as South America, East and North Africa and China. The pathology of the disease is mainly due to the physical pressure exerted on the intermediate host's viscera by the developing hydatid cyst which contains larval worms and protoscoleces (Klotz et al., 2000).

The three approaches available for the treatment of this pathology are the surgery, the PAIR (puncture-aspiration-injection-reaspiration) percutaneous protocol and chemotherapy.

Success rates of the systemic chemotherapy depend on the cyst content and the agent used. Benzimidazoles such as albendazole (ABZ) and its sulphoxide derivative, albendazole sulphoxide (ABZ-SO), are the most preferred drugs employed in the disseminated disease, in inoperable cases and for prophylaxis before surgery (Horton, 1989, 1997; Bartoloni et al., 1992).

Benzimidazole anthelmintics drugs are effective against nematodes, cestodes and trematodes. The intrinsic effect of these compounds on the parasite relies on a subsequent alteration of basic cell functions as a result of their binding to parasite tubulin and leading to a disruption of the tubulin-microtubule dynamic equilibrium (Lacey, 1990). ABZ is more active *in vitro* than the other benzimidazoles and has improved gastrointestinal absorption and bioavailability as well as reports of better clinical results. However, the lack of water solubility is an important physicochemical parameter for the formulation of the highly potent benzimidazoles, namely, ABZ, fenbendazole, mebendazole or ABZ-SO (Smego and Sebanego, 2005;

* Corresponding author. Present address: Laboratoire de Physico-Chimie des Systèmes Polyphasés, UMR CNRS 8612 – IFR 141, Université Paris-Sud, 5 rue J.B. Clément, 92296 Châtenay-Malabry, France. Tel.: +33 1 46 83 54 65; fax: +33 1 46 83 53 12.
E-mail address: vincent.faivre@u-psud.fr (V. Faivre).

0378-5173/$ – see front matter © 2007 Elsevier B.V. All rights reserved.
doi:10.1016/j.ijpharm.2007.11.040

Senyuz et al., 2001; Saimot, 2001). In the case of ABZ, in order to prepare solutions, different approaches have been investigated during the last decade. Since ABZ is basic in nature, its solubility could be notably increased by ionisation in an acid medium, although this rise is not enough for the preparation of high ABZ concentration (Garcia et al., 2003). It is also possible to go up its water solubility by the use of surfactants, for instance, polysorbate, bile salts or cosolvents (Transcutol®) (Torrado et al., 1996; Redondo et al., 1998). Unfortunately, the absorption enhancer effects described with the previous molecules are generally correlated to an irritation of the digestive mucosa. A similar approach was also used with hydroxypropyl-β-cyclodextrin (Garcia et al., 2003). Alternatively, the ABZ solubility could be improved by formulation of solid dispersion with polyvinylpyrrolidone (Daniel-Mwambete et al., 2004) or poly-lactic acid nanoparticles (Rodrigues et al., 1995).

In reality, after oral administration, ABZ is converted by first-pass hepatic metabolism into its less active metabolite, ABZ-SO, that achieves variable concentrations in blood, bile, liver tissue, cyst fluid and wall, or crosses the blood-brain barrier (Smego and Sebanego, 2005; Senyuz et al., 2001; Saimot, 2001; Lanusse et al., 1998).

The basic structure of the hydatid cyst was described as follows. The cyst is filled with hydatid cyst fluid which contains both protoscoleces and host-derived proteins, and surrounded by a two-layered hydatid cyst wall. The innermost layer of this structure is the live parasite tissue, named germinal layer, which is a few cell bodies wide from which small packets of protoscoleces bud into the cyst lumen. This layer lays down around it an extensive (1–2 mm thick), acellular, carbohydrate-rich, mechanically resistant structure named laminated layer (Klotz et al., 2000). That supportive and defense structure protects the cyst from direct attack by host immune cells (Diaz et al., 2000).

The success of the chemotherapeutic treatment of hydatid disease is based upon the capacity of the drug to operate on the germinal layer and the protoscolices of the hydatid cyst interior at adequate concentrations for sufficient periods. To reach this goal, two of the most important parameters are the drug diffusion trough the cyst membrane and the drug concentration in the cyst environment. From this point of view, in the present work, we have confronted the cyst membrane with classical permeation method to clarify the drug physicochemical parameters required to allow good drug diffusion towards the hydatid cyst interior. Because of the benzimidazole low aqueous solubility, dyes have been used as model molecules. Then, we decided to formulate benzimidazole-loaded nanoparticles in order to increase the apparent solubility of the drug and to avoid its hepatic metabolism. Furthermore, it is well known that after parenteral administration, a massive accumulation of nanoparticles could be observed in the liver and lungs (Soppimath et al., 2001; Moghimi and Szebeni, 2003). These two tissues being the most frequent resident niches of the hydatid cyst in humans, benzimidazole-loaded nanoparticles seem to be promising forms for the treatment of hydatosis.

2. Materials and methods

2.1. Materials

Congo red, tartrazine and erythrosine were purchased from Kuhlmann R.A.L. Carminic acid and gentian violet were provided by Cooper. ABZ (ABZ) and poly(D,L-lactide) (PLA, molecular weight 90,000–120,000) were purchased from Sigma–Aldrich. Methanol and acetonitrile were provided by Prolabo. Acetic acid, sodium periodate (99%), acetone and poly(vinyl alcohol) (PVA, molecular weight 13,000–23,000, 87–89% hydrolysed) were obtained from Carlo Erba, Acros organics, Merck and Fluka, respectively.

All the solvents used without further purification were of analytical grade.

2.2. Albendazole sulphoxide synthesis

ABZ-SO was prepared as reported (De Laurentis et al., 1996).

Three grams of $NaIO_4$ was added in 250 ml of a methanol–water (1:1) mixture in a two-necked flask. This mixture has been stirred at room temperature until a complete dissolution of the $NaIO_4$. Then a solution made up of 3 g of ABZ and 60 ml of acetic acid has been added from a dropping funnel. After 24 h of stirring, the mixture was checked by thin layer chromatography and filtrate under vacuum. Then, a 50% solution of NaOH was slowly added to pH 7. The solution turned cloudy due to the formation of a precipitate. Three hundred millilitres of water has been incorporated to avoid the precipitation of AcONa and stirred weakly during 1 h. The suspension was filtered under vacuum and the filtrate was evaporated in order to eliminate methanol. An ice bath was used to digest the filtrate and to obtain a second precipitate which was filtrate under vacuum. Similar by thin layer chromatography, the two precipitates were washed several times with water. The raw material was dried under vacuum until a constant weight was reached. Impurities (ABZ sulphone and salt) were removed by silica gel column chromatography eluting with a mixture dichloromethane–methanol (95:5).

The product was analyzed by the determination of the melt point, infra-red spectroscopy, high-performance liquid chromatography (HPLC) and nuclear magnetic resonance spectroscopy (^{1}H-NMR and ^{13}C-NMR).

2.3. Nanoparticle preparation

The particles were obtained by an emulsion solvent evaporation method. D,L-Polylactide (50 mg) and the drug (ABZ or ABZ-SO, 5 mg) was dissolved in 5 ml of acetone. The solution was added dropwise under magnetic stirring (900 rpm) for 10 min with an aqueous phase (10 ml) containing 100 mg of poly(vinyl alcohol). The preparation was homogenized by a 13000 rpm stirring with an Ultra-turrax®. After filtration (Isopore membrane, 0.5 μm), acetone and water were evaporated under vacuum and the volume of the preparation was adjusted to 5 ml.

ABZ aqueous suspension and unloaded nanospheres were prepared by the same procedure, omitting polymer and ABZ, respectively.

Rhodamine B-labelled nanoparticle suspension was prepared following a similar procedure using of 4.5 mg Rhodamine B base in place of ABZ in the acetone. 1ml of the obtained suspension was washed by water, filtered through an Ultrafree®-CL filter unit (Filter Ultrafree®-CL, pore size 0.1 μm, Millipore, Bedford, USA) and subjected for 30 min centrifugation (1500 g) to remove free fluorescent material.

2.4. Determination of the dye molecular descriptors

The following parameters have been used to characterized the molecular properties of the studied dyes: the molecular weight, M_w, the octanol–water partition coefficient, log P, the number of hydrogen bond acceptors, $N_{acceptor}$, and donors, N_{donor}, the number of rotatable bonds, $N_{rotation}$, and the molecular polar surface area, PSA.

All these parameters have been calculated using the Molinspiration property calculator software (Molinspiration Cheminformatics, Bratislava, Slovak Republic). Log P is calculated by a methodology taking into account sum of fragment-based contributions and correction factors. The number of rotatable bonds is a simple topological parameter which describes the molecular flexibility. Rotatable bond is defined as any single non-ring bond, bounded to non-terminal heavy (i.e., non-hydrogen) atom. Amine C–N bonds are not considered because of their high rotational energy barrier (ca. 20–22 kcal/mol). The molecular polar surface area calculation is based on a methodology published by Ertl et al. (2000) as a sum of fragment contributions. O- and N-centered polar fragments are also considered.

2.5. Hydatid cyst removal

The membranes of hydatid cysts were obtained from infected sheep. At autopsy, the hepatic cysts were macroscopically localized. A punction of hydatid fluid was made and the cyst was open. The membranes of fertile cysts were taken off and kept at −80 °C in a 10% DMSO (cryoprotectant) aqueous solution until use.

2.6. Ex vivo permeation studies through hydatid cyst membranes

Before use, excised hydatid cysts were incubated three times at room temperature in saline solution (0.9% NaCl) to remove impurities. Hydatid cyst membrane samples (around 2 cm^2) were cut carefully with a scalpel and mounted onto static Franz glass diffusion cells containing 9 ml of saline solution (inner face of the cyst membrane in contact with the receptor compartment). Because of the low solubility of the drug, the saline solution has been supplemented with 3% of ovalbumin during the experiment with ABZ. The diffusion area was 0.79 cm^2. The receptor compartment was stirred with a magnetic bar at 37 ± 0.2 °C throughout the study. Mounted membranes were kept onto diffusion cells for 1 h before treatment. A 0.5 ml sample of 1% dye aqueous solution, free-ABZ aqueous suspension or ABZ-loaded nanoparticle suspension was then deposited onto hydatid cyst membrane. After 0.25, 0.5, 0.75, 1, 2, 3, 4, 5, 6 and 24 h, 0.5 ml sample of receptor fluids were removed and replaced by the same volume of fresh solution. The concentration of dyes or ABZ in the receptor fluids was assayed by the analytical methods below described.

2.7. Quantification of dye amounts

The determination of the dye concentrations in the receptor compartment was obtained by simple UV–visible spectrophotometric measurements using a systronics model 106A digital spectrophotometer. The concentration linearity ranges were [1.2–39 μg/ml], [2.4–160 μg/ml], [1.2–20 μg/ml], [1.2–39 μg/ml], and [0.6–9.8 μg/ml] for tatrazine, carminic acid, gentian violet, congo red and erythrosine, respectively, with squared correlation coefficient, r^2, above 0.999 for all tested molecules. The receptor solution samples could be diluted to reach the previous ranges.

2.8. Permeation result analysis

The permeation results have been treated with the Fick's first law of diffusion:

$$J = \frac{dQ}{dt} \times \frac{1}{A} = \frac{K_s \times D}{h} \times \Delta C \quad (1)$$

where J is the drug flux, dQ/dt is the amount of dye diffused per unit of time, A is the treated membrane surface area, K_s is the partition coefficient, D is the diffusion coefficient, h is the diffusional path length and ΔC is the concentration gradient of dye.

Then the permeability coefficient, P, was determined by the following equation:

$$P = \frac{J}{C_0} \quad (2)$$

where C_0 is the dye concentration in the donor compartment.

2.9. Intra- and inter-variability of the weight of different cyst membrane samples

The variability of sample weights was used to approach the variability of the diffusional path length, h. After removal with a 6 mm diameter punch, five samples of three different cysts were weighted. The intra- and inter-cyst variation coefficients were then determined.

2.10. Quantification of drug loading

Because of their different water solubility, two procedures have been used to determine the drug loading: ABZ was quantified inside particles and ABZ-SO outside.

The obtained ABZ nanoparticle suspension was filtered through a 5 μm Millex®-SV membrane (Milipore, Bedford,

USA) to eliminate precipitates formed during preparation due to its poor aqueous solubility. Entrapment efficiency is calculated as follow:

2.10.1. ABZ loading

$$\text{ABZ entrapment efficiency (\%)} = \frac{(\text{ABZ}_{\text{total}} - \text{ABZ}_{\text{free}})}{\text{ABZ}_{\text{initial}}} \times 100$$

in which, $\text{ABZ}_{\text{total}}$ is the concentration of drug in the final nanoparticle suspension (loaded and soluble unloaded ABZ). ABZ_{free} is the amount of soluble unloaded ABZ in the suspension. $\text{ABZ}_{\text{initial}}$ is the initial amount (5 mg) of ABZ used to prepare the ABZ particles. Owing to the very low water solubility, the soluble unloaded ABZ is negligible. Then, the loading efficiency can be approximately calculated as follow:

$$\text{ABZ entrapment efficiency (\%)} = \frac{\text{ABZ}_{\text{total}}}{\text{ABZ}_{\text{initial}}} \times 100$$

2.10.2. ABZ-SO loading

After the preparation, the ABZ-SO loaded nanoparticles were purified by ultracentrifugation. The preparations were divided in aliquots of 1.5 ml and centrifuged at 25000 rpm during 30 min at 4 °C. After re-suspension, the particles were re-centrifuged. Finally, three centrifugations were made on each aliquot. The amount of drug entrapped into nanoparticles was calculated by difference between the initial amount of drug and the amount of free ABZ-SO by the following relation:

$$\text{ABZSO entrapment efficiency (\%)} = \frac{(\text{ABZSO}_{\text{initial}} - \text{ABZSO}_{\text{supernatant}})}{\text{ABZSO}_{\text{initial}}} \times 100$$

in which, $\text{ABZSO}_{\text{initial}}$ is the initial amount (5 mg) of ABZ-SO for formulation and $\text{ABZSO}_{\text{supernatant}}$ is the sum of ABZ-SO amounts quantified in the three supernatants.

2.11. Particle shape determination

The morphological examination of nanoparticles was performed using a transmission electron microscope JEM-1200 EX from JEOL (Japan). The negative staining was obtained with a 4% sodium phosphotungstate solution (pH 7.2) on carbon-parlodion grids.

2.12. Quantification of drug amounts

The drug amount (ABZ or ABZ-SO) was assayed by high-performance liquid chromatography (HPLC) with a Hewlett Packard 1050 series HPLC system (Germany), an isocratic pump and an automatic sampler. For the two investigated drugs, the column was an Inerstil ODS-3 (5 μm, 4.6 mm × 250 mm, OAI6069) from GL Sciences Inc. (Japan). The other HPLC parameters depend on the drug of interest. For ABZ, the mobile phase was a methanol–water (75:25) mixture. Sample volume injected was 50 μl. The flow rate was settled at 0.8 ml/min and the detection was performed at 291 nm. The retention time was 10.6 min and for concentrations between 0 and 20 μg/ml, peak area increases were linear with a squared correlation factor, r^2, of 0.9999. Concerning the ABZ-SO, the mobile phase was a mixture of acetonitrile–water–85% phosphoric acid (200 ml:800 ml:188 μl). Sample volume injected was 30 μl. The flow rate was 1.0 ml/min and the detection was performed at 290 nm. The retention time was 7.5 min and for concentrations between 0 and 50 μg/ml, peak area increases were linear with a squared correlation factor, r^2, higher than 0.9999.

2.13. Particle size analysis

The mean particle size and the size distribution of nanoparticles were estimated by light scattering (dispersant refractive index = 1.33; detector angle = 90°; wavelength = 670 nm) with a Zetamaster® II (Malvern Instruments, Orsay, France). To estimate the stability at 4 °C, the measurements were made immediately and during 60 days following preparation. Before measurements, the nanoparticles suspensions were diluted in deionised water.

2.14. Particle zeta potential

The measurements of zeta potential were performed using the technique of electrophoretic laser Doppler anemometry with a Zetamaster® II (Malvern Instruments, Orsay, France). The determinations were carried on in three different media: deionised water and HEPES buffer (pH 7.4, NaCl 150 mM) supplemented or not with 10% (v/v) of fetal bovine serum.

2.15. Distribution of fluorescent probe across cyst germinal membrane

Hydatid cyst germinal membrane was mounted onto Franz static diffusion cell and 0.5 ml of rhodamine B base-labelled nanoparticle suspension or ABZ aqueous suspension was added to the donor compartment. The receptor compartment comprised of 9 ml of ovalbumine saline solution was maintained at 37 °C and stirred with a magnetic bar. After 24 h the membrane was removed from the diffusion cell, residual formulation was removed by washing with distilled water. The membrane was then examined by using a confocal laser scanning microscope (Leica-SP2, Mannheim, Germany; gain 1.000, excitation and emission wavelengths: 514 and 522 nm, pinhole: 121 μm). All images were acquired with identical settings.

2.16. Permeation studies across whole cyst membrane

The entire hydatid cysts were incubated in either rhodamine B-loaded nanoparticle suspension or ABZ-loaded nanoparticle suspension. After 3 h, the cysts were taken out and punctured by a needle to aspirate the intra-cystic media. These media were then subjected for microscopic study and ABZ assay, respectively.

2.17. Statistical analysis

Statistical calculations were executed using the Kaleidagraph tools (Synergy software). Comparisons were analyzed by using one-way ANOVA with post hoc testing using Bonferroni's correction. Except if noted, the chosen level of significance was

Table 1
Molecular descriptors of the studied dyes

Dye	M_w (g/mol)	Log P	$N_{acceptor}$	N_{donor}	$N_{violation}$	PSA (Å^2)	$N_{rotation}$
Gentian violet	372.5	2.64	3	0	0	9.5	4
Tartrazine	465.5	−0.47	13	1	1	217.3	6
Carminic acid	492.4	−0.99	13	9	2	242.5	3
Congo red	650.7	5.09	12	4	3	215.9	7
Erythrosine	833.9	4.33	5	0	1	93.4	2

The underlined values are out of the "rule of five" ranges (see text).

$P<0.05$ or $P<0.01$. As the group were small ($n=3$), normal distribution was assumed and not further tested.

3. Results and discussion

3.1. Physicochemical properties of the dyes

The properties of the dyes are described in the Table 1. It is important to note that the obtained molecular descriptor values, especially the partition coefficient, are comparable with values expressed in chemical databases (http://chemdb.niaid.nih.gov, http://hmdb.med.ualberta.ca and http://cdb.ics.uci.edu). For each studied parameter, some dye describing values are higher than the generally admitting limits between important and poor permeation abilities. Thus, a set of rules imposing limitations on log P, molecular weight, and number of hydrogen bond donors and acceptors introduced by Lipinski has become particularly popular in the field of membrane permeation prediction (Lipinski et al., 1997). These limitations are known as the "rule of five" because each border value deals with 5. The rule states that poor absorption and permeation are more likely when: there are more than 5 H-bond donors, the molecular weight is over 500, the log P is over 5 and there are more than 10 H-bond acceptors. However, the compound classes that are substrates for biological transporters are exceptions to the rule.

Molecular polar surface area (PSA), i.e., surface belonging to polar atoms, is a descriptor that was shown to correlate well with passive molecular transport through membranes as Caco-2 layer or blood-brain barrier and to allow prediction of transport properties of drug (Veber et al., 2002). With the chosen dyes, a large range of PSA was investigated, from 9.5 to 242.5 Å^2. Navia and Chaturvedi (1996) suggested the importance of the molecular flexibility, quantified by the $N_{rotation}$ parameter, for example in the case of the digestive absorption.

3.2. Permeation coefficient

The permeation coefficient values are summarized in the Table 2. In a previous work, Garcia-Llamazares et al. studied the membrane permeability of secondary hydatid cyst to ABZ-SO by incubation of whole cysts in a drug-containing medium (Garcia-Llamazares et al., 1998). In spite of the different methodology, the authors obtained ABZ-SO permeation coefficients between 0.56×10^{-5} and 0.81×10^{-5} cm/s depending on the treated or untreated state of the cysts. In the present study, the permeation coefficients of the dyes are in a similar range, from 0.27×10^{-5} to 1.52×10^{-5} cm/s.

Table 2
Values of the dye permeation coefficient

Dye	Permeation coefficient (cm/s) $\times 10^{-5}$
Gentian violet	1.14 ± 0.50
Tartrazine	0.62 ± 0.46[a]
Carminic acid	0.27 ± 0.25[b,c]
Congo red	1.31 ± 0.47[c]
Erythrosine	1.52 ± 0.08[a,b]

The curve fitting was conducted for each individual diffusion experiment, and data represent the mean ± standard deviation of three or four determinations.
[a] $p<0.01$.
[b] $p<0.05$.
[c] $p<0.05$.

Except for erythrosine, the permeation standard deviations are relatively important (variation coefficients from 5 to 93% depending on the dye). Several parameters dealing with the experimental method or with the membrane state could explain such important variation coefficients. First, the membrane of the hydatid cyst is irregular in thickness. The weight of cyst membrane samples having similar surface area is summarized in the Table 3. The inter-cyst variation coefficient is around 30% confirming morphological differences among cysts. In addition, a similar intra-cyst variation coefficient should be noted, suggesting membrane thickness variations even in a same cyst. With the Franz cells we used in the present experiments, an approach to overcome this problem was to normalize the results by the weight of each membrane sample as classically made with skin for example. Actually, the cyst membrane was thin and very easily damaged, it was not possible to manipulate the same sample for the weighting and the permeation experiments. It is evident from the Eqs. (1) and (2) that a change of sample weight, corresponding to the change of the membrane thickness, modifies the diffusional path length, h, as well as the permeation coefficient. However, Garcia–Llamazes and co-authors, who worked

Table 3
Weight intra- and inter-variations of hydatid cyst membrane samples

Cyst 1	5.6 ± 1.2 mg (21.6%)
Cyst 2	9.8 ± 2.6 mg (26.5%)
Cyst 3	10.0 ± 3.3 mg (33.0%)
Inter-cyst variation coefficient	30%

Data represent the mean ± standard deviation of three (inter-cyst variation) or five (intra-cyst variation) determinations.

with whole cysts and avoided the intra-cyst variation, obtained variation coefficient from 29 to 46% (Garcia-Llamazares et al., 1998). Besides the inter-cysts membrane thickness fluctuations, these authors observed permeation coefficient differences due to the past of the cysts. Indeed, they noted a loss of cyst permeability to ABZ-SO following its treatment with Netobimin. Furthermore, Xiao et al. (1992) observed a significantly decrease of the glucose content in the hydatid fluid of cysts from mice treated with mebendazole after intravenous glucose administration, suggesting that mebendazole had an inhibitory effect on the transport of exogenous glucose to the cyst wall. Similarly, the stage of development, the maturation and the localization of the cysts would also alter their permeation properties (Holcman and Heath, 1997).

3.3. Permeation coefficient versus dye descriptors

With our results, no linear relationship between permeation coefficient and the $N_{rotation}$, polar surface area, and $N_{violations}$ parameters could be observed (figures not shown, correlation coefficients, r, lower than 0.68), suggesting that these molecular descriptors could not be used as simple diffusion predictive factor. Contrary to the previous ones, the permeation coefficient correlates closely with the partition coefficient log P ($r = 0.951$, $P < 0.05$) as described in Fig. 1. From the present results, it is possible to propose a simple model in order to determine the diffusion of molecule through the hydatid cyst membrane. Thus, the permeation coefficient, P, could be estimated from the partition coefficient, log P, by using the following equation:

$$P = 5.98 \times 10^{-6} + 1.77 \times 10^{-6} \times \log P \quad (3)$$

In their study, Garcia-Llamazares et al. (1998) measured a permeation coefficient equal to $8.06 \times 10^{-6} \pm 2.30 \times 10^{-6}$ cm/s for the ABZ-SO diffusion through untreated hydatid cyst membrane (Garcia-Llamazares et al., 1998). With the Eq. (3), and using the partition coefficient calculated with the molinspiration tools (log $P = 1.60$), the calculated permeation coefficient of the ABZ-SO is equal to 8.81×10^{-6} cm/s. These two permeation coefficients are remarkably similar.

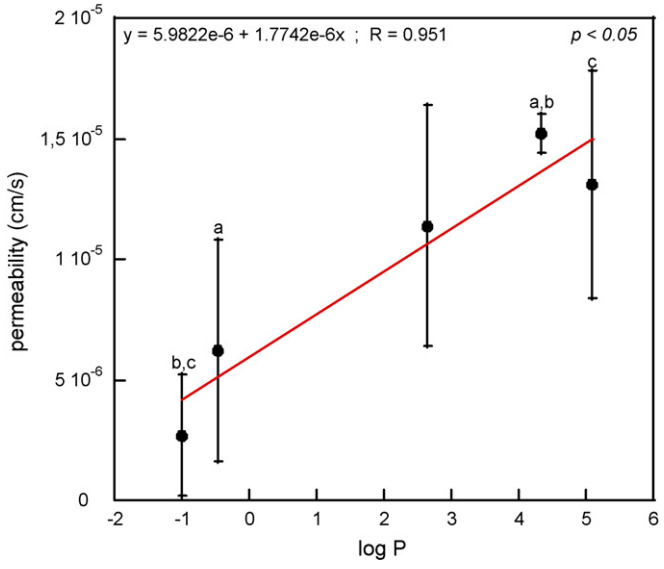

Fig. 1. Permeation coefficients vs. partition coefficient, log P, of the studied dyes with linearization established by the Kaleidagraph tools (Synergy software).

Our results confirm the preponderant role played by the lipophilicity of the anthelmintic drugs and the barrier function of the cyst germinal layer. By considering the general diffusion routes, the laminated and germinal layer model provides an interesting structural base for the understanding of the relevant molecule transport process across the cyst wall. Compounds are able to move due to their thermic energy in the direction of a concentration gradient (passive diffusion). Passive diffusion through a biomembrane may occur via its lipid structures (transcellular pathway) or in its water-filled pores (inter-, para-cellular pore or tight junction pathway) (Camenisch et al., 1996). The log P dependence of the dye diffusion strongly suggests a transcellular pathway through the lipid structures instead of along aqueous pores. The laminated layer of the cyst wall is made up of a number of acellular laminations and besides giving support to the cyst, it is presumed to protect the parasite from the host's immune responses. It consists of a protein-polysaccharide complex with a carbohydrate component that builds up with glucose, galactose, glucosamine and galactosamine. If these carbohydrates could protect the parasite from the immune response of the host, probably inhibiting complement activation, they could not be a barrier for the diffusion of hydrophilic molecules due to their important polarities. Contrary to the previous one, the germinal layer is made of undifferentiated proliferative totipotential cells, which produce brood capsules projecting into the lumen of the mother cysts. This lipid-rich syncytium would certainly favour the diffusion of lipophilic molecules (important log P) and drastically reduce the diffusion of the more hydrophilic ones (negative log P).

Mottier et al. (2003) reported a high correlation between molecular lipid solubility (expressed as log P) and the availability (expressed as Area Under Curve) of benzimidazole compounds within the helminth parasite used as a model (*Moniezia benedeni*). In their study, the total drug amount recovered in *Moniezia benedeni* increases linearly with the octanol–water partition coefficient with a correlation coefficient, r, equal to 0.87. With a similar approach Alvarez et al. (2001) described the more important total ABZ recovered in *Ascaris suum* and *Fasciola hepatica* compared with ABZ-SO. The authors explained such difference by the fact that a lipophilic drug as ABZ may have a greater capability to across the external surface of the parasite than its more polar sulphoxide metabolite. Traditionally, the nematode's cuticle, the cestode's tegument and the hydatid cyst membrane have been considered to be barriers limiting entry of molecules into the parasite. However, among others (Geary et al., 1995; Reisin et al., 1977), the two last cited works and the present report confirm that the passive diffusion could be a major route of entry for substances in parasite tissues.

In the specific case of the hydatid cyst wall, as the log P of the most important benzimidazole drugs is comprised between 2 and 4 (Mottier et al., 2003), corresponding to a permeation coefficient around 1×10^{-5} cm/s (Fig. 1), the penetration of the drugs into the cyst will not constitute a limiting factor for the

Table 4
Characterization results of the unloaded and loaded nanoparticles

	Unloaded particles	ABZ-loaded particles	ABZSO-loaded particles
Mean size (nm)			
After preparation	194.6 ± 14.4	288.2 ± 10.8	197.5 ± 13.9
After 15 days	185.6 ± 6.4	278.2 ± 11.6	212.8 ± 13.2
After 60 days	225.2 ± 29.1	322.6 ± 42.9	205.4 ± 29.1
Zeta potential (mV)			
In water	−5.7 ± 1.5	−9.7 ± 1.6	−14.8 ± 4.7
In HEPES buffer	−3.0 ± 0.3	−2.7 ± 1.2	−2.3 ± 1.2
In FBS medium	−6.8 ± 0.3	−3.6 ± 1.4	−4.5 ± 1.3
Entrapment efficiency (%)	–	36.4 ± 6.4	6.4 ± 5.1

Data represent the mean ± standard deviation of three determinations.

their effectiveness. By way of contrast, the passive diffusion is governed by the concentration gradient across the membrane of interest (Eqs. (1) and (2)). Because of their poor water solubility (Dayan, 2003), leading to a low concentration gradient, the benzimidazole flux should be reduced. To optimize the anthelmintic therapy, the challenge is now to increase this concentration gradient with appropriate formulations.

3.4. Nanoparticle characterization

The characterization results have been summarized in the Table 4. The size of the particles is around 200 nm, from 194.6 to 288.2 nm, depending on the loaded-drug. The weak increase of size (and standard deviation) observed for each formulation after 2 months is not statistically significant ($P < 0.05$). This stability of size suggests the absence of matrix surface erosion and the good physicochemical stability of our nanoparticles in storage conditions despite a quite low zeta potential. The spherical shape of the nanoparticles has been clearly observed with microscopy as described in the Fig. 2. Furthermore, the micrographs seem to confirm the mean size increase obtained with ABZ-loaded particles in comparison with ABZ-SO-loaded one.

Highly negative zeta potential values, around −20 to −30 mV, are expected for pure polyester nanoparticles thanks to the presence of the carboxyl groups on the polymeric chain extremities (Quintanar-Guerrero et al., 1996; Konan et al., 2003). In the present work, the zeta potential values tend to zero in rapport with the residual PVA chains on the nanoparticle surface. Leading to a shield between the nanoparticle surface and the surrounding medium, PVA would mask the carboxyl groups existing on the particle surface (Konan et al., 2003). During the process of preparation, it has been frequently described that drug could be adsorb on nanoparticles. This adsorption has often explained zeta potential fluctuations. ABZ and ABZ-

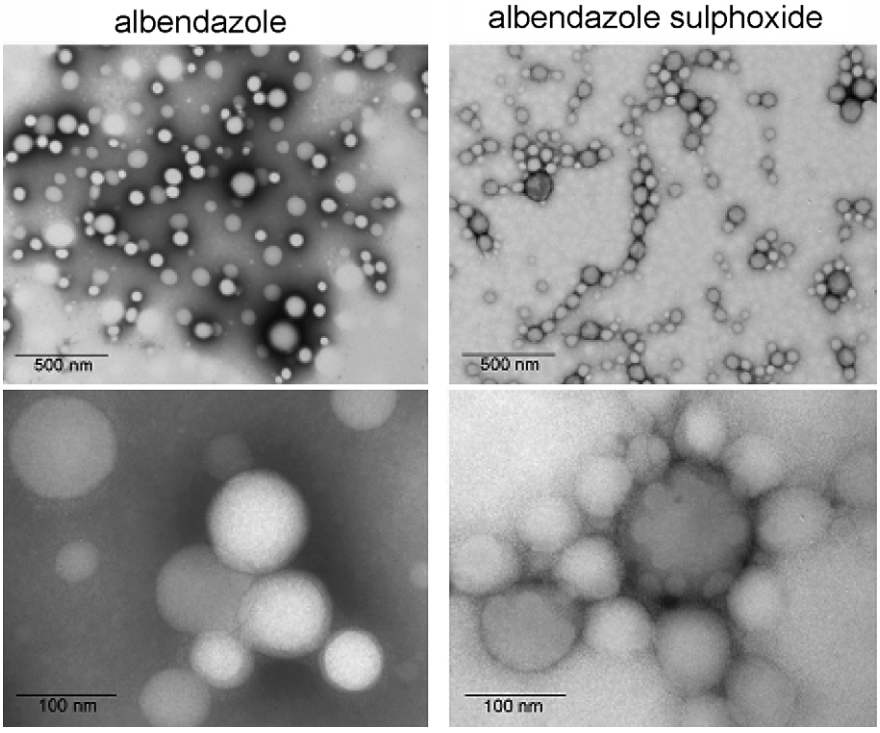

Fig. 2. Transmission electron microscopy pictures of the nanoparticles.

SO are amphoteric molecule where the protonation steps are well separated from each other ($\Delta \log K > 4$). Thus, the pK_a values of ABZ are 3.37 and 9.93 and then, only the neutral form will be present from pH 5.4 to 7.9. Furthermore, Botsoglou et al. (1997) described that ABZ-SO is a free base form for pH between 4.7 and a superior limit higher than 7.4. More recently, Wu et al. (2005), proposed a more accurate model concerning the ABZ-SO ionisation steps: the molecule will be protonated on the amine group in position 1 for pH values inferior to 3.5 and the deprotonation occurs on the amine group in position 3 at pH higher than 9.8. Then, at the two studied pH, ABZ and ABZ-SO mostly remain in non-ionised states. Moreover, a pH decrease would lead to protonation of the position 1 amine group and then the surface charge would increase.

It is interesting to note the absence of quantitative masking effect due to our drugs in their neutral forms, suggesting the absence of drug adsorption on the particle surface.

The entrapment efficiencies of the two drugs are completely different: it is six times more important with ABZ in relation to its sulphoxide metabolite (Table 4). As ABZ-SO is more soluble in a 1% PVA solution than ABZ (640 μg/ml versus 1.3 μg/ml), we could assume that an important amount of ABZ-SO has been solubilized in the aqueous phase during the emulsification step of the nanoparticle preparation process.

For the drug release studies, only ABZ-loaded nanoparticles have been investigated for essentially three reasons, (i) the more important entrapment efficiency obtained with this drug, (ii) the more important log *P* of ABZ, leading to a better diffusion through the cyst membrane (see above) and (iii) the higher therapeutic efficacy described with ABZ in the literature (Smego and Sebanego, 2005; Senyuz et al., 2001; Saimot, 2001).

3.5. Permeation studies across cyst membrane

The Fig. 3 describes the ABZ permeation through hydatid cyst membrane from ABZ-loaded nanoparticles in comparison with a free ABZ suspension by using vertical Franz cells. Despite of an important variability (probably due membrane thickness differences as suggested in the previous parts of this paper), an increase of the drug in the receptor compartment could be observed in the case of the nanoparticles. This could be probably explained by the better dispersion of the drug obtained with nanoparticles compared with raw suspensions.

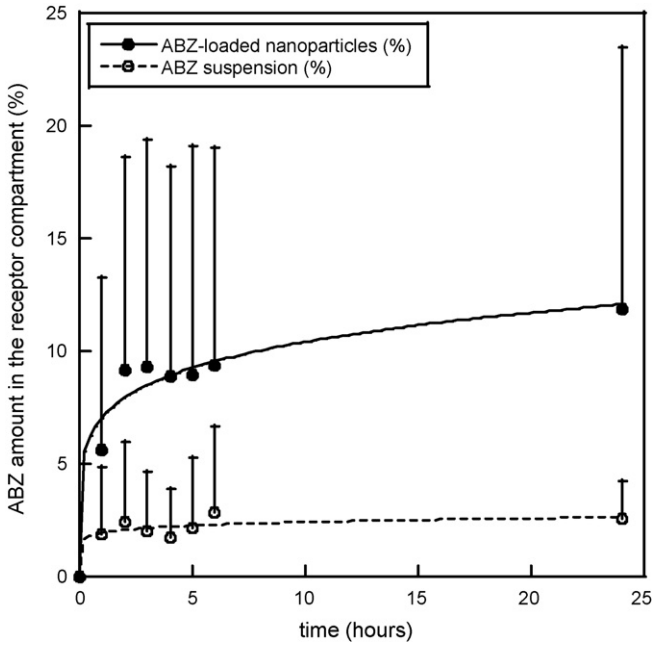

Fig. 3. *In vitro* delivery of albendazole from albendazole-loaded nanoparticles and raw albendazole suspension through hydatid cyst membranes.

To complete this experiment, whole cysts were incubated in ABZ-loaded nanoparticle suspension during 3 h. After that time, the cysts were washed, punctured by a needle to aspirate the intra-cystic media and the drug quantified in it. After three hours of incubation, the intra-cystic ABZ concentration was

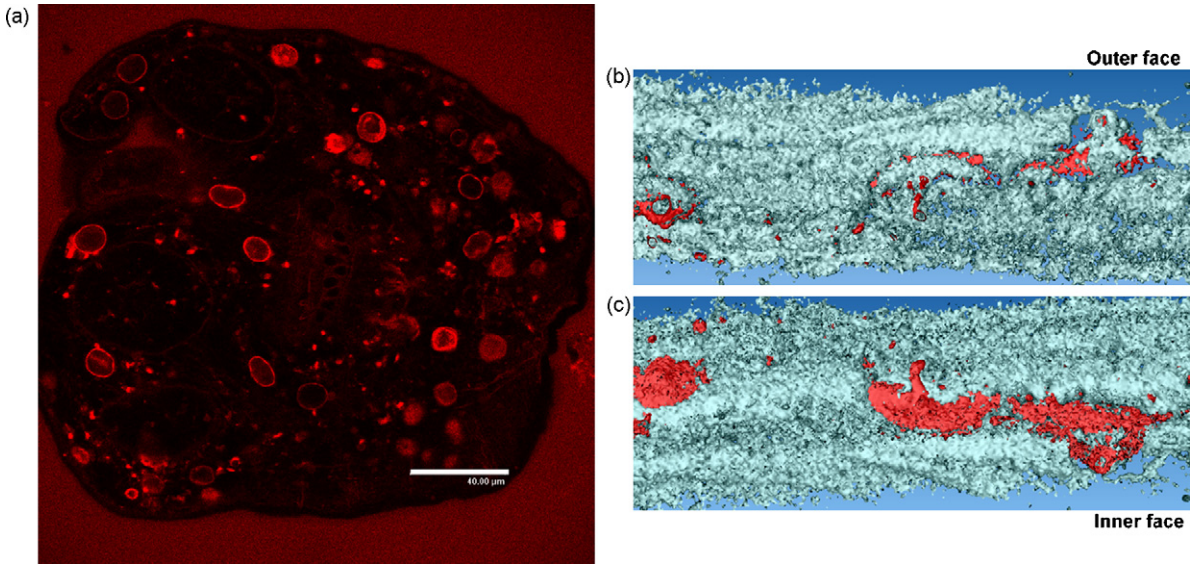

Fig. 4. Confocal microscopy pictures describing *Echinococcus granulosus* scolex penetrated by rhodamine B base (a) and rhodamine B base heterogeneous accumulation in the outer (b) and inner (c) face of the hydatid cyst membrane.

1 ± 0.5 μg/ml. A similar incubation was used with rhodamine-loaded nanoparticles. Such fluorescent dye was used as model molecule to follow the drug accumulation in the cyst. The cyst liquid (Fig. 4a) and the cyst membrane (Fig. 4b and c) were then observed with confocal microscopy. After the 3 h incubation with rhodamine B base-loaded nanoparticles, the intra-cystic media was coloured in red, due to rhodamine B. Moreover, there were many protoscoleces labelled with the fluorescent dye. Reconstructed confocal microscopy (Fig. 4b and c) suggests important knowledge concerning our system. First there is an important accumulation of fluorescent probe in the membrane. As a matter of fact, this retention seems to take place extensively in the inner layer of the membrane as shown the red colour distribution in the Fig. 4b and c. This accumulation in the innermost layer confirms the role of diffusion controlling barrier played by the germinal layer of the cyst wall as concluded after the dye permeation experiments. In addition, in a same plan, the co-existence of coloured and uncoloured regions should be noted. This heterogeneous distribution evokes an accumulation of the nanoparticles in particular region of the cyst wall rather than a simple diffusion of the dye which generally leads to continuous layer of fluorescence. In reality, we have shown that during the incubation time (3 h), approximately 35% of the encapsulated rhodamine B is able to leave the nanoparticle (data not shown) and from the confocal microscopy picture, it is not possible to discriminate the loaded nanoparticles and the free rhodamine B.

It is interesting to note that the success of the chemotherapeutic treatment of hydatid disease requires the ability of the drug to operate on the germinal layer and on the protoscoleces of the hydatid cyst interior at adequate concentrations (Morris, 1987). By considering rhodamine B base as a model drug of benzimidazole (similar log *P* range) (Mottier et al., 2003), these two goals are clearly reached. *In vitro*, effective concentration of intra-cystic ABZ is 0.1 μg/ml (Morris et al., 1987). This concentration is largely obtained *in vitro* with ABZ-loaded nanoparticles (1 μg/ml after a 3 h incubation).

4. Conclusion

The diffusion of several model molecules through the hydatid cyst membrane has been described in this report. The permeation coefficients correlate closely with the octanol–water partition coefficient of the studied compounds: the more lipophilic they are, the more important is their diffusion. This penetration behaviour confirms the role of diffusion barrier played by the innermost layer of the cyst wall (germinal layer). The preparation of benzimidazole-loaded nanoparticles seems interesting for the treatment of hydatid cyst, especially in the case of ABZ. Indeed, this drug has a good encapsulation rate and an interesting partition coefficient. In comparison with a simple drug suspension, we observed a significant increase of the drug diffusion from the formulation to the interior of the cyst. This passive diffusion through the hydatid cyst membrane was favoured by the important log *P* of ABZ as concluded in the first part of this paper and by the increase of the ABZ apparent solubility with regard to the nanoparticle form.

Thanks to the liver accumulation after nanoparticles injection and the good candidate of ABZ for a passive diffusion through the cyst wall, ABZ-loaded nanoparticles seem to be promising forms for the treatment of the hydatidosis. Therefore, the *in vivo* behaviour of these nanoparticles should be investigated to complete the present work.

Acknowledgments

The authors would like to thank S. Peyrol and Y. Tourneur for their help in transmission electron microscopy and confocal microscopy, respectively, and C. Morel.

References

Alvarez, L.I., Mottier, M.L., Sanchez, S.F., Lanusse, C.E., 2001. *Ex vivo* diffusion of ABZ and its sulphoxide metabolite into *Ascaris suum* and *Fasciola hepatica*. Parasitol. Res. 87, 929–934.

Bartoloni, C., Tricerri, A., Guidi, L., 1992. The efficacy of chemotherapy with mebendazole in human cystic echinococcosis: long-term follow-up of 52 patients. Ann. Trop. Med. Parasitol. 86, 249–256.

Botsoglou, N.A., Fletouris, D.J., Psomas, I.E., Mantis, A.I., 1997. Retention behaviour of the sulphoxide, sulphone and 2-aminosulphone metabolites of ABZ in ion-pair liquid chromatography. Anal. Chim. Acta 354, 115–121.

Camenisch, G., Folkers, G., van de Waterbeemd, H., 1996. Review of theoretical passive drug absorption models: historical background, recent developments and limitations. Pharm. Acta Helv. 71, 309–327.

Daniel-Mwambete, K., Torrado, S., Cuesta-Bandera, C., Ponce-Gordo, F., Torrado, J.J., 2004. The effect of solubilization on the oral bioavailability of three benzimidazole carbamate drugs. Int. J. Pharm. 272, 29–36.

Dayan, A.D., 2003. ABZ, mebendazole and praziquantel. Review of non-clinical toxicity and pharmacokinetics. Acta Trop. 86, 141–159.

De Laurentis, N., Milillo, M.A., Crescenzo, G., Bruno, S., 1996. A new synthetic method of the main ABZ metabolites. Pharm. Pharmacol. Lett. 6, 51–53.

Diaz, A., Ibarguren, S., Breijo, M., Willis, A.C., Sim, R.B., 2000. Host-derived annexin II at the host-parasite interface of the *Echinococcus granulosus* hydatid cyst. Mol. Biochem. Parasitol. 110, 171–176.

Ertl, P., Rohde, B., Seizer, P., 2000. Fast calculation of molecular polar surface area as a sum of fragment-based contributions and its application to the prediction of drug transport properties. J. Med. Chem. 43, 3714–3717.

Garcia, J.J., Bolas, F., Torrado, J.J., 2003. Bioavailability and efficacy characteristics of two different oral liquid formulations of ABZ. Int. J. Pharm. 250, 351–358.

Garcia-Llamazares, J.L., Alvarez-de-Felipe, A.I., Redondo-Cardena, P.A., Pieto Fernandez, J.G., 1998. *Echinococcus granulosus* membrane permeability of secondary hydatid cysts to ABZ sulphoxide. Parasitol. Res. 84, 417–420.

Geary, T.G., Blair, K.L., Ho, N., Sims, S.M., Thompson, D.P., 1995. Biological functions of nematode surfaces. In: Bothroyd, J.C., Komuniecki, R. (Eds.), Molecular Approaches to Parasitology. Wiley-Liss, New-York, pp. 57–76.

Holcman, B., Heath, D.D., 1997. The early stages of *Echinococcus granulosus* development. Acta Trop. 64, 5–17.

Horton, R.J., 1989. Chemotherapy of *Echinococcus* infection in man with ABZ. Trans. R. Soc. Trop. Med. Hyg. 83, 97–102.

Horton, R.J., 1997. ABZ in treatment of human cystic echinococcosis: 12 years of experience. Acta Trop. 64, 79–93.

Klotz, F., Nicolas, X., Debonne, J.-M., Garcia, J.-F., Andreu, J.-M., 2000. Kystes hydatiques du foie. Encycl. Med. Chir., 7-023-A-10, 16p.

Konan, Y.N., Cerny, R., Favet, J., Berton, M., Gurny, R., Alléman, E., 2003. Preparation and characterization of sterile sub-200 nm meso-tetra(4-hydroxylphenyl)porphyrin-loaded nanoparticles for photodynamic therapy. Eur. J. Pharm. Biopharm. 55, 115–124.

Lacey, E., 1990. Mode of action of benzimidazoles. Parasitol. Today 6, 112–115.

Lanusse, C.E., Virkel, G.L., Sanchez, S.F., Alvarez, L.I., Lifschitz, A.L., Imperiale, F., 1998. Ricobendazole kinetics and availability following subcutaneous

administration of a novel injectable formulation to calves. Res. Vet. Sci. 65, 5–10.

Lipinski, C.A., Lombardo, F., Dominy, B.W., Feeney, P.J., 1997. Experimental and computational approaches to estimate solubility and permeability in drug discovery and development settings. Adv. Drug Deliv. Rev. 23, 3–25.

Moghimi, S.M., Szebeni, J., 2003. Stealth liposomes and long circulating nanoparticles: critical isues in pharmacokinetics, opsonization and protein-binding properties. Prog. Lipid Res. 42, 463–478.

Morris, D., 1987. Pre-operative ABZ therapy for hydatid cyst. Br. J. Surg. 74, 805–806.

Morris, D., Chinnery, J.B., Ubhi, C., 1987. A comparison of the effects of ABZ, its sulphone metabolite, and mebendazole on the viability of protoscoleces of *Echinococcus granulosus* in an *in vitro* culture system. Trans. R. Soc. Trop. Med. Hyg. 81, 804–806.

Mottier, M.L., Alvarez, L.I., Pis, M.A., Lanusse, C.E., 2003. Transtegumental diffusion of benzimidazole anthelmintics into *Moniezia benedeni*: correlation with their octanol–water partition coefficients. Exp. Parasitol. 103, 1–7.

Navia, M.A., Chaturvedi, P.R., 1996. Design principles for orally bioavailable drugs. Drug Discov. Today 1, 179–189.

Quintanar-Guerrero, D., Fessi, H., Allémann, E., Doelker, E., 1996. Influence of stabilizing agents and preparative variables on the formation of poly(D,L-lactic acid) nanoparticles by an emulsification-diffusion technique. Int. J. Pharm. 143, 133–141.

Redondo, P.A., Alvarez, A.I., Garcia, J.L., Villaverde, C., Prieto, J.G., 1998. Influence of surfactants on oral bioavailability of ABZ based on the formation of the sulphoxide metabolites in rats. Biopharm. Drug Dispos. 19, 65–70.

Reisin, I.L., Rabito, C.A., Rotunno, C.A., Cereijido, M., 1977. The permeability of the membranes of experimental secondary cysts of *Echinococcus granulosus* to [^{14}C] mebendazole. Int. J. Parasitol. 7, 189–194.

Rodrigues, J., Bories, C., Emery, I., Fessi, H., Devissaguet, J., Liance, M., 1995. Development of an injectable formulation of ABZ and *in vivo* evaluation of its efficacy against Echinococcus multilocularis metacestode. Int. J. Parasitol. 25, 1437–1441.

Saimot, A.G., 2001. Medical treatment of liver hydatidosis. World J. Surg. 25, 15–20.

Senyuz, O.F., Yesildag, E., Celayir, S., 2001. ABZ therapy in the treatment of hydatid liver disease. Surg. Today 31, 487–491.

Smego, R.A., Sebanego, P., 2005. Treatment options for hepatic cystic echinococcosis. Int. J. Infect. Dis. 9, 69–76.

Soppimath, K.S., Aminabhavi, T.M., Kulkarn, A.R., Rudzinski, W.E., 2001. Biodegradable polymeric nanoparticles as drug delivery devices. J. Control. Release 70, 1–20.

Torrado, S., Torrado, S., Cadorniga, R., Torrado, J.J., 1996. Formulation parameters of ABZ solution. Int. J. Pharm. 140, 45–50.

Veber, D.F., Johnson, S.R., Cheng, H.-Y., Smith, B.R., Ward, K.W., Koppie, K.D., 2002. Molecular properties that influence the oral bioavailability of drug candidates. J. Med. Chem. 45, 2615–2623.

Wu, Z., Razzak, M., Tucker, I.G., Medlicott, N.J., 2005. Physicochemical characterization of ricobendazole. I. Solubility, lipophilicity, and ionization characteristics. J. Pharm. Sci. 94, 983–993.

Xiao, S.H., You, J.Q., Guo, H.F., Feng, J.J., Sun, H.L., Jiao, P.Y., Yao, M.Y., Chai, J.J., 1992. Effect of mebendazole on glucose uptake of *Echinococcus granulosus* cyst. Acta Pharmacol. Sin. 13, 473–477.